

Supplemental Material

Local nucleosome dynamics and eviction following a double-strand break are reversible by NHEJ-mediated repair in the absence of DNA replication

Vinay Tripuraneni¹, Gonen Memisoglu², Heather K MacAlpine¹, Trung Tran³, Wei Zhu¹, Alexander J Hartemink³, James E Haber², and David M MacAlpine^{1*}

¹Department of Pharmacology and Cancer Biology

Duke University Medical Center, Durham, NC 27710

²Department of Biology and Rosenstiel Basic Medical Sciences Research Center

Brandeis University, Waltham, MA 02454

³Department of Computer Science

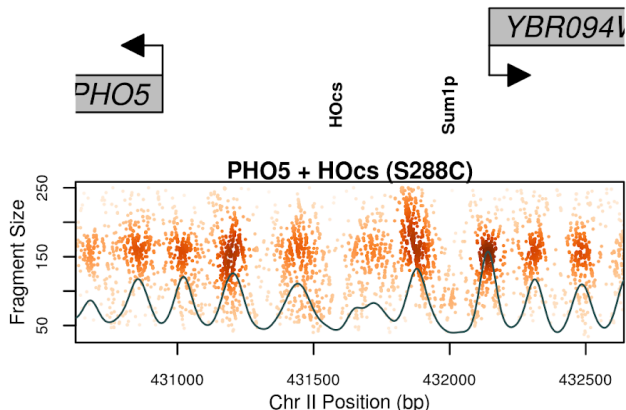
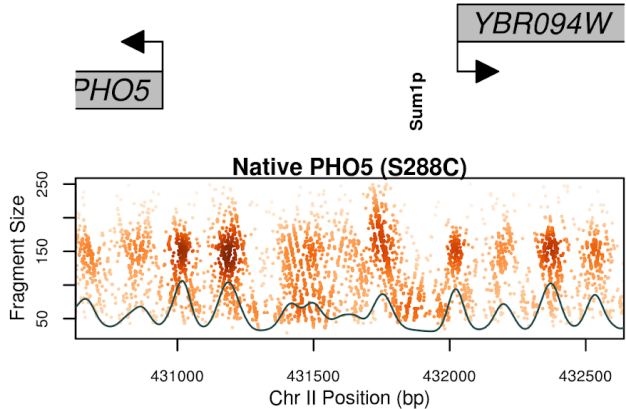
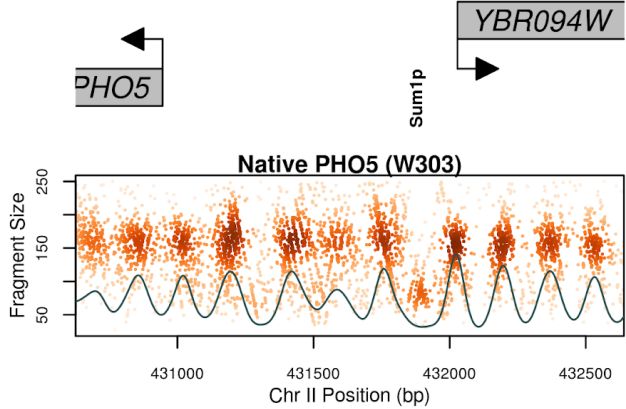
Duke University, Durham, NC 27708

Supplemental Data and Figures

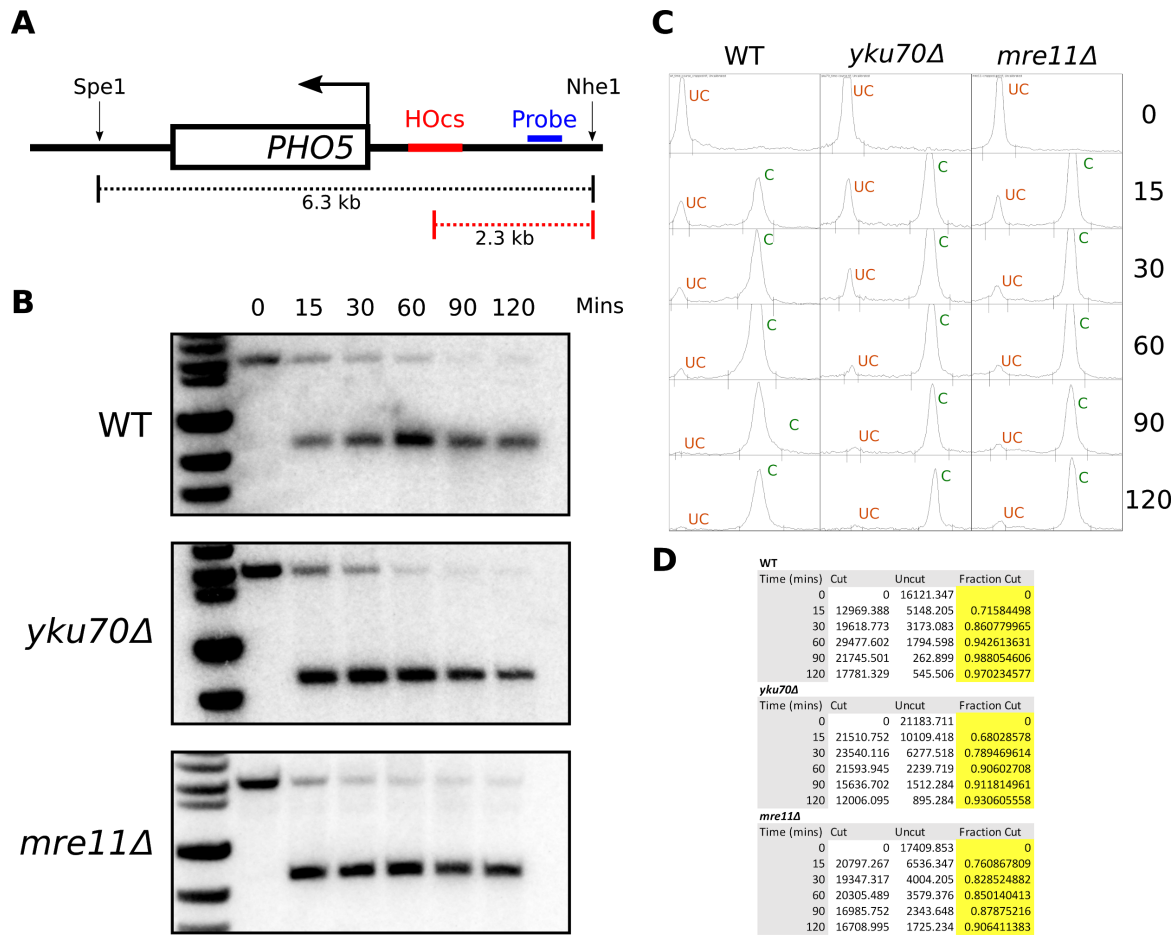
Supplemental Table 1. Oligonucleotide sequences.

| | |
|------------------------------|--|
| Pho5_southern_f | <i>TTTCACACCCTCCATTGTCA</i> |
| Pho5_southern_r | <i>TTTGGGGCACATAAGGATTC</i> |
| DNL4-ko-f | <i>AATAAAAATCTAGAACTGAAGGAAATAGTA ACGGATTATTTAGGTcagattgtactgagagtgc</i> |
| DNL4-ko-r | <i>GTATTAATAAACTTCAAAAAATTAAGCCTC CGCAAAACGCACCAccttacgcatctgtgcgg</i> |
| YKU70-ko-f | <i>AGCTATGATTTGTTAAGTGAAGTCTAAGCCTG ATTTTAAAACGGGAATATTcggcacagagcaga ttgta</i> |
| YKU70-ko-r | <i>CTACCAAATATTGTATGTAACGTTATAGATA TGAAGGATTTCAATCGTCTctgatgcggtattttctc ct</i> |
| MRE11-ko-f | <i>GCAGACAATTGACGCAAGTTGTACCTGCTCA GATCCGATAAAACTCGACTcggcacagagcaga ttgta</i> |
| MRE11-ko-r | <i>AAGCCCTTGTTATAAATAGGATATAATATA ATATAGGGATCAAGTACAActgatgcggtattttct cct</i> |
| Pho5-gRNA-f | <i>GTGTCGCACGCTCTCTTTACGTTTT</i> |
| Pho5-gRNA-r | <i>GTAAAGAGAGCGTGCGACACGATCA</i> |
| Pho5_HOcs_CRISPR-Cas9_gBlock | <i>GACCTGATGTCAGTCCCCACGCTAATAGCG GCGTGTGCGCAGATCTAAATAAATTCGTTTTC AATGATTAAAATAGCATAGTCGGGTTTTTCT TTTAGTTTTAGCTTTCCGCAACAGTATAATT TTATAAACCCCTGGTTTTGGTTTTGTAGAGTG GTTTCGCTCTTTTACAGGACGCCGGAGACC GGCATTACAAGGA</i> |

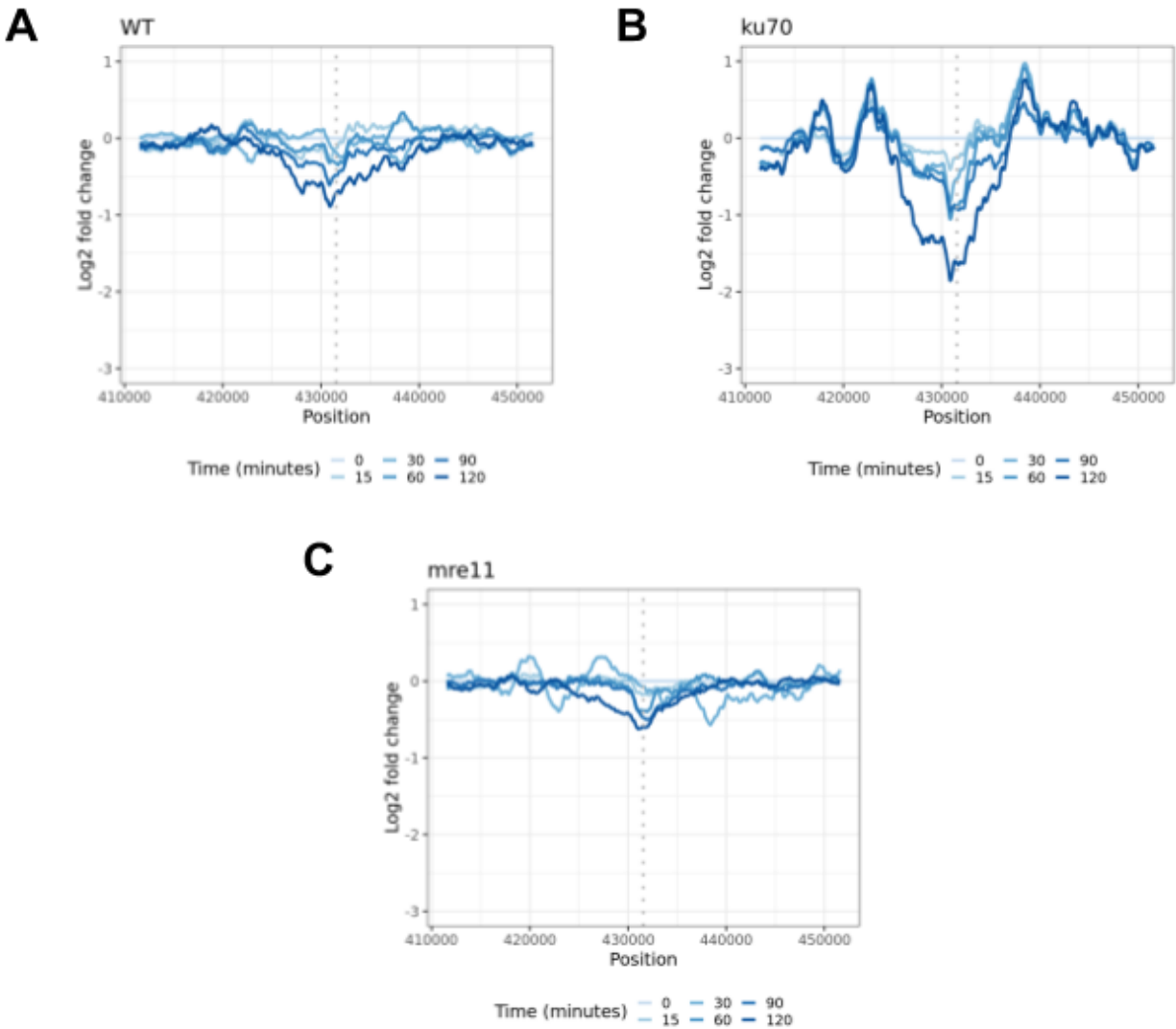
Supplemental Table 2. Summary statistics of sequencing libraries and concordance data for replicate experiments. See `Supplemental_Table_S2.xlsx`.



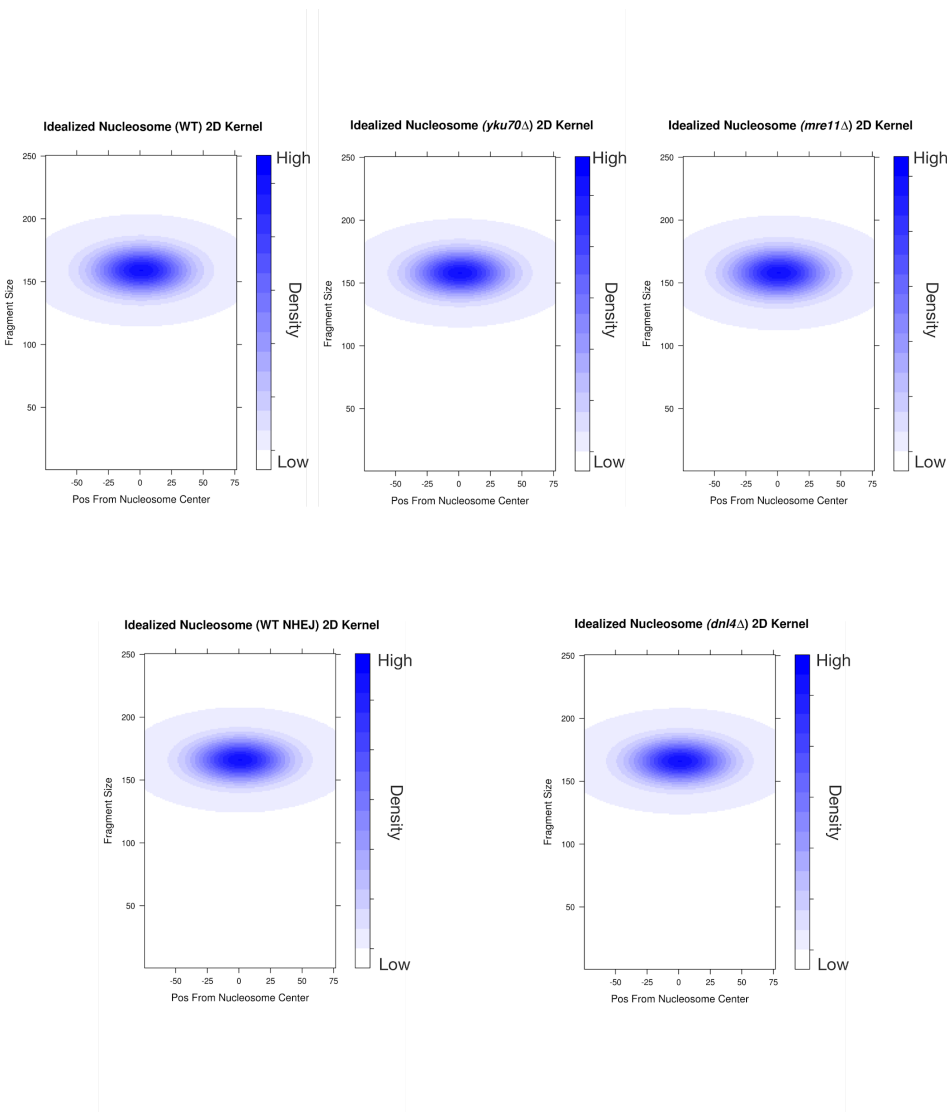
Supplemental Figure 1. Structure of the *PHO5* locus prior to and after the HOcs insertion. Top panel is the native *PHO5* locus from the W303 yeast strain background while the middle panel is the same locus in the JKM139 strain, which is largely derived from S288C. The bottom panel is the S288C strain with the HOcs insertion. The +1 nucleosome of *PHO5* is the 4L nucleosome in **Figure 1A**.



Supplemental Figure 2. Southern Blotting of WT, *yku70Δ*, and *mre11Δ* strains. **A.** Schematic of the southern blotting probe and the detected fragment sizes at the *PHO5* locus with the 117 bp HO recognition site. **B.** Southern blots of the 3 strains profiled in this study. **C.** Line profiles of each lane that were analyzed in ImageJ to extrapolate uncut (UC, orange) and cut (C, green) band intensity. **D.** Table of the data obtained from the analysis in **C**, fraction cut is determined by dividing the cut signal by the sum of the uncut and cut signals.

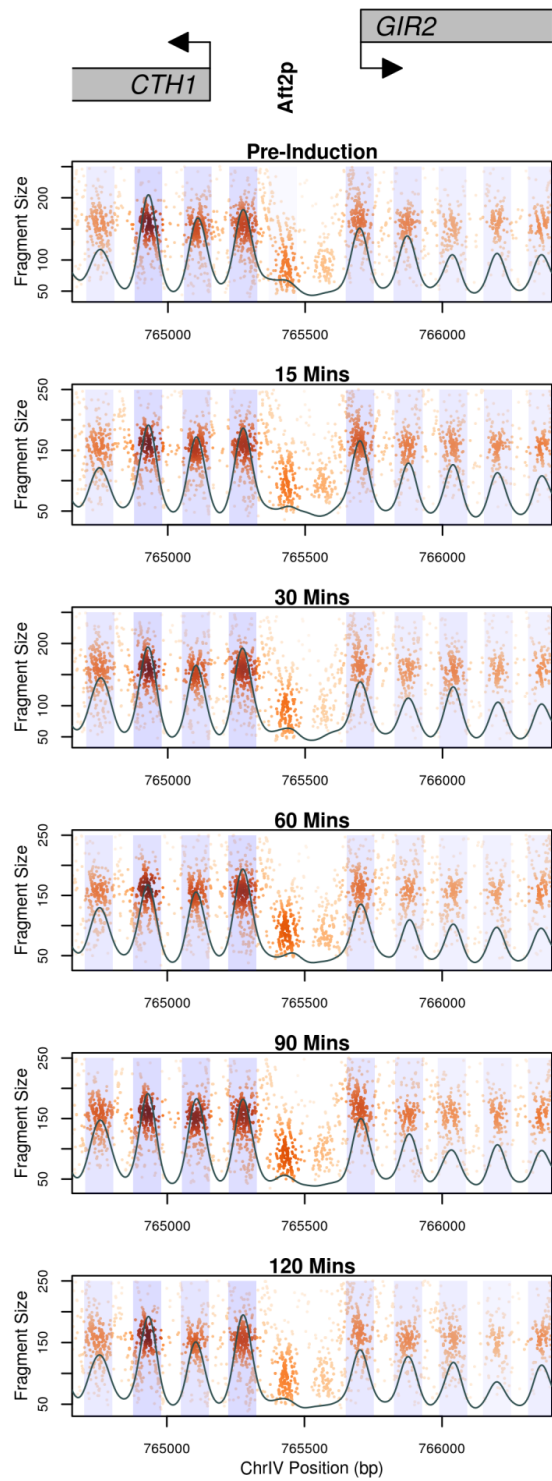


Supplemental Figure 3. DNA resectioning surrounding the HO induced break at the *PHO5* locus. Total DNA was recovered and the relative copy number was assessed for each timepoint by high throughput sequencing. Panels A, B, and C represent WT, *yku70* Δ and *mre11* Δ strains. Greater time post-induction (min) is plotted in darker shades of blue indicated below each plot.

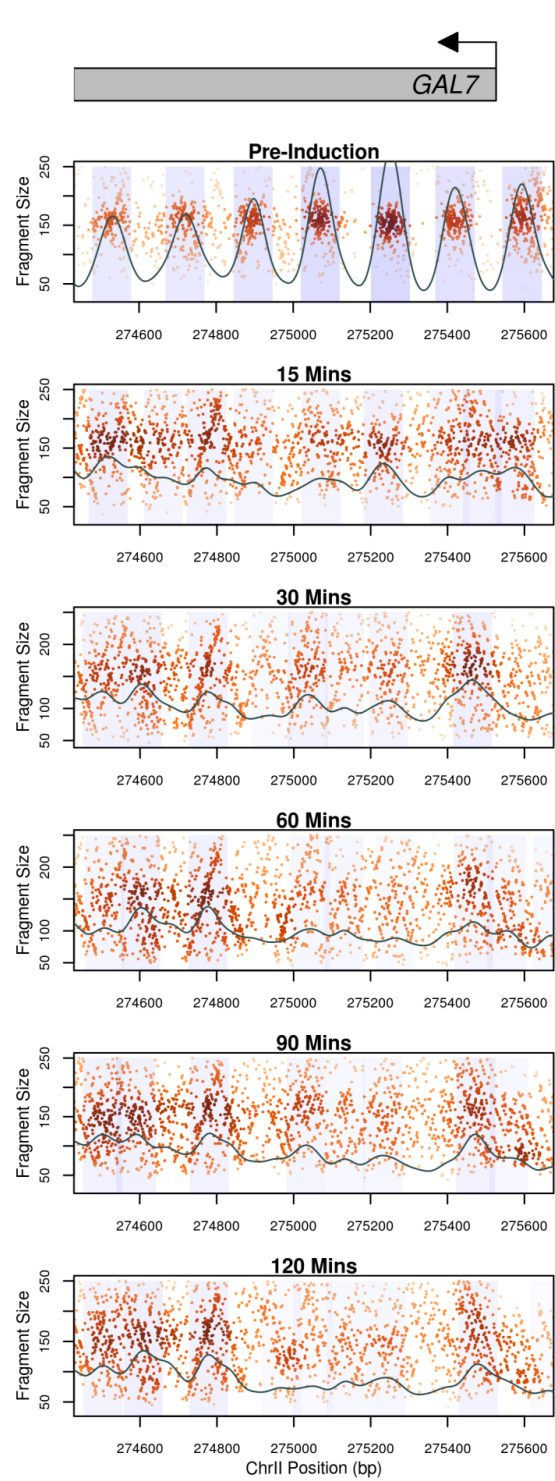


Supplemental Figure 4. Idealized two-dimensional density (2D) kernel of nucleosomes derived from the pre-induction sample for each time-course. The size and fragment distribution parameters for this nucleosome were derived from analyzing the 8,632 nucleosomes chemically mapped (Brogaard et al. 2012) on Chr IV for each experiment which were similar across all experiments.

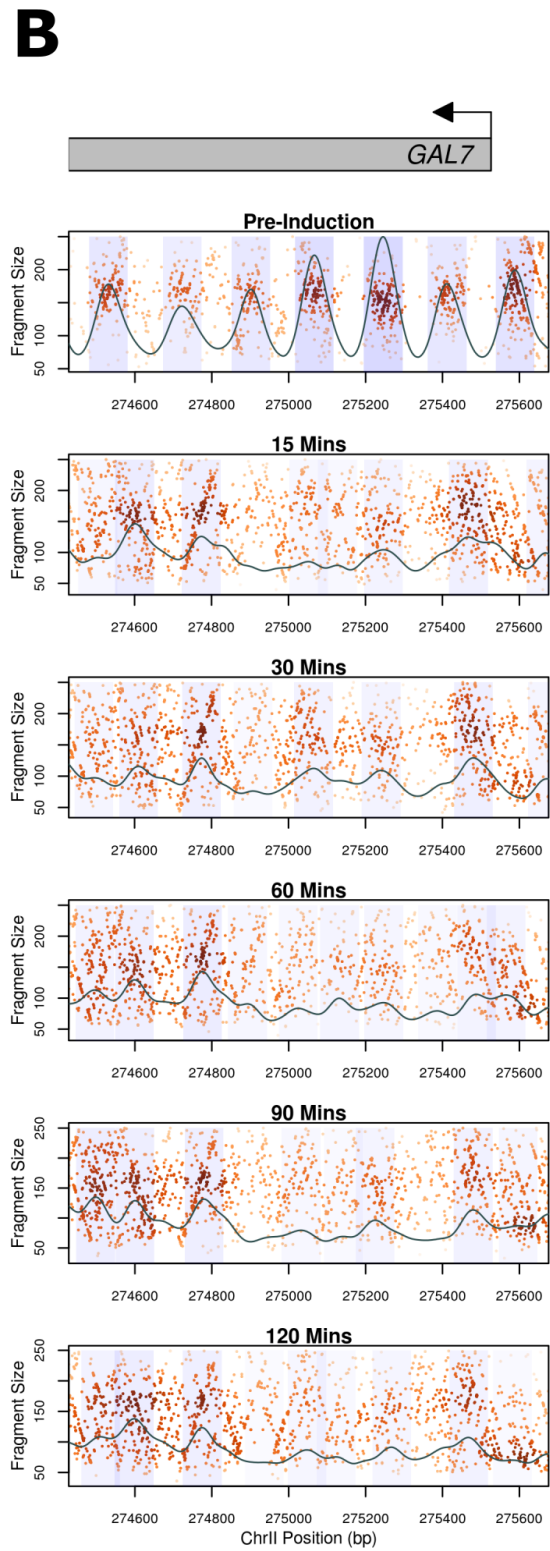
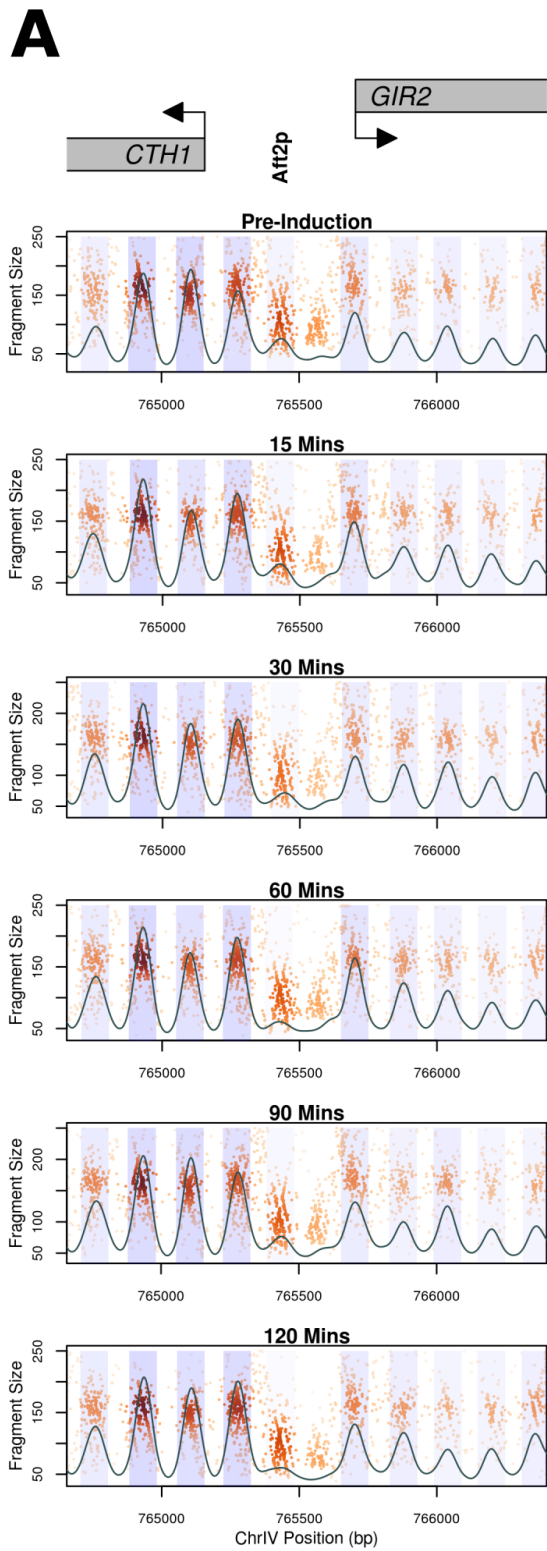
A



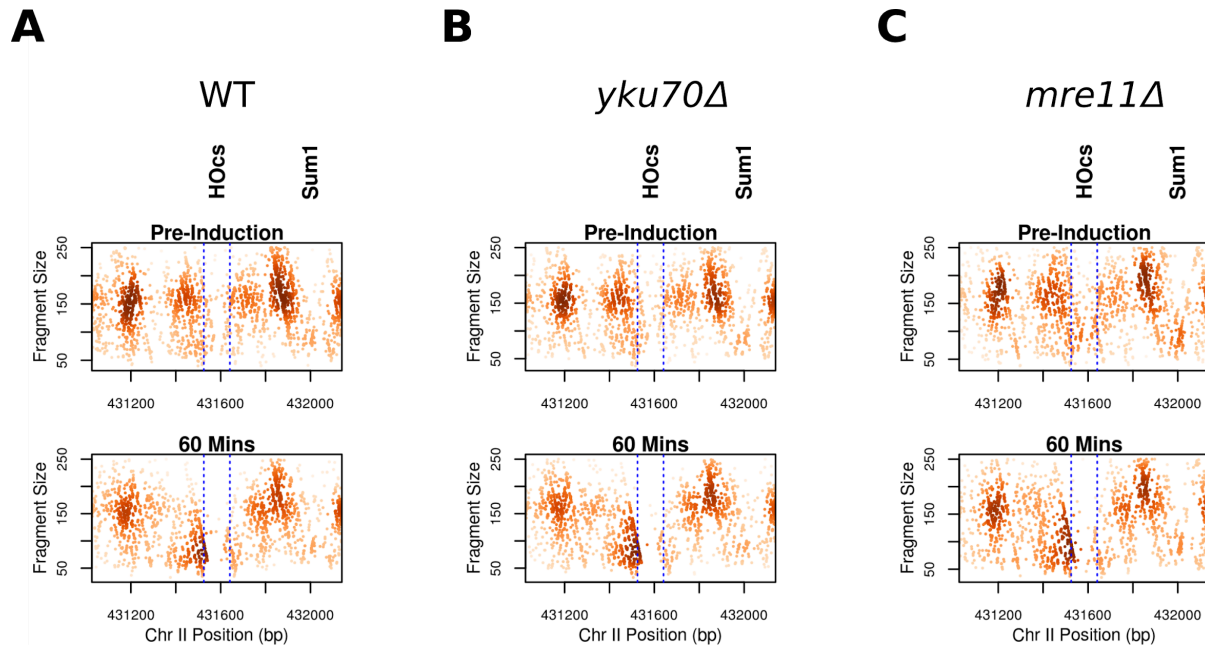
B



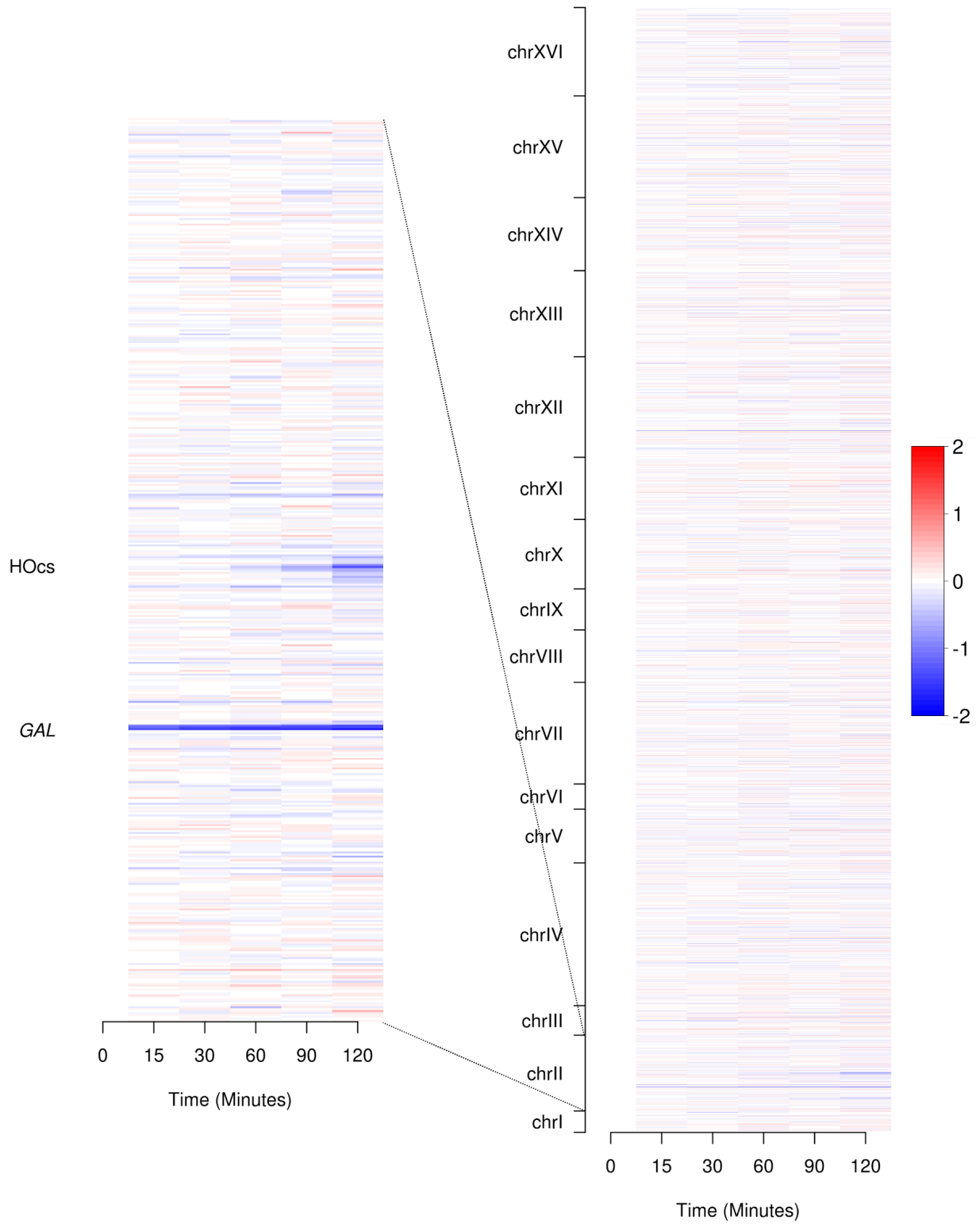
Supplemental Figure 5. *yku70Δ* control loci genome wide chromatin occupancy profiles (GCOPs). **A.** GCOP for the *CTH1* and *GIR2* loci which serve as a control for unaltered chromatin. Gray boxes depict gene bodies, with arrows indicating the direction of transcription. The bold vertical text indicates the Aft2p binding site between these two genes. A two-dimensional cross correlation with an idealized nucleosome (see Methods) is calculated at every base pair and depicted as a continuous black trace. The peaks of this cross-correlation analysis represent the most likely position of a locally detected nucleosome and we have shaded +/- 0.5 standard deviations of nucleosome position from the center of each detected peak. The intensity of the shaded color is proportional to the cross-correlation score of the nucleosome peak. **B.** GCOP for the *GAL7* locus following galactose induction.



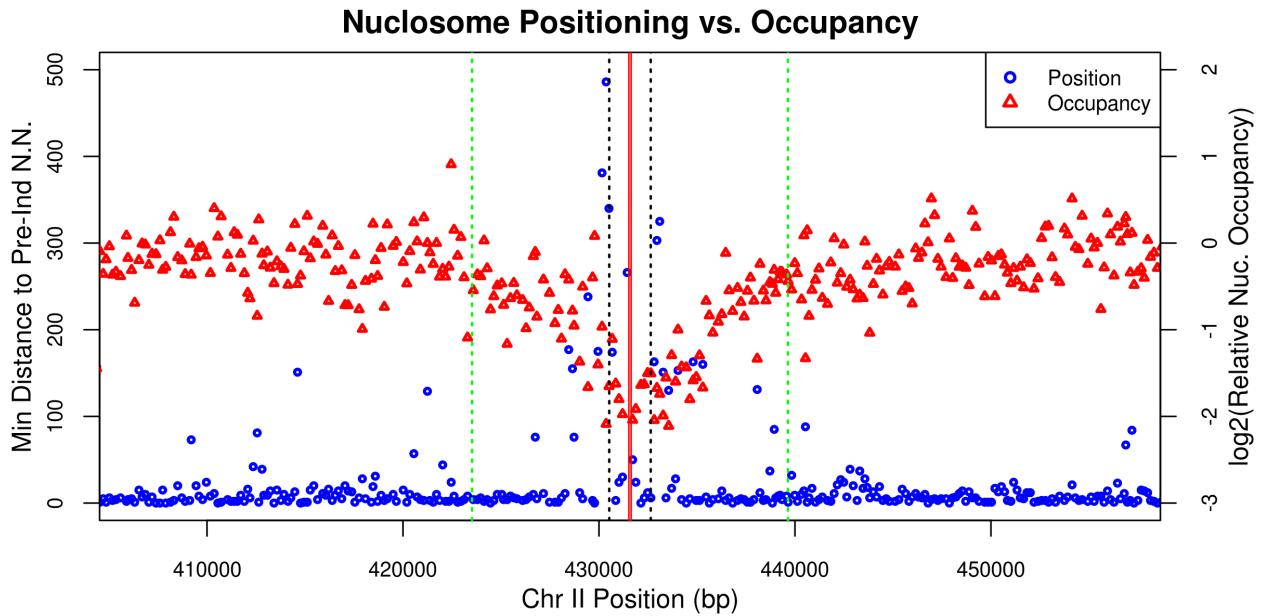
Supplemental Figure 6. *mre11Δ* control loci genome wide chromatin occupancy plots (GCOPs) **A.** GCOP for the *CTH1* and *GIR2* loci which serve as a control for unaltered chromatin. Gray boxes depict gene bodies, with arrows indicating the direction of transcription. The bold vertical text annotates the Aft2p binding site between these two genes. A two-dimensional cross correlation with an idealized nucleosome (see Methods) is calculated at every base pair and depicted as a continuous black trace. The peaks of this cross-correlation analysis represent the most likely position of a locally detected nucleosome and we have shaded +/- 0.5 standard deviations of nucleosome position from the center of each detected peak. The intensity of the shaded color is proportional to the cross-correlation score of the nucleosome peak. **B.** GCOP for the *GAL7* locus following galactose induction.



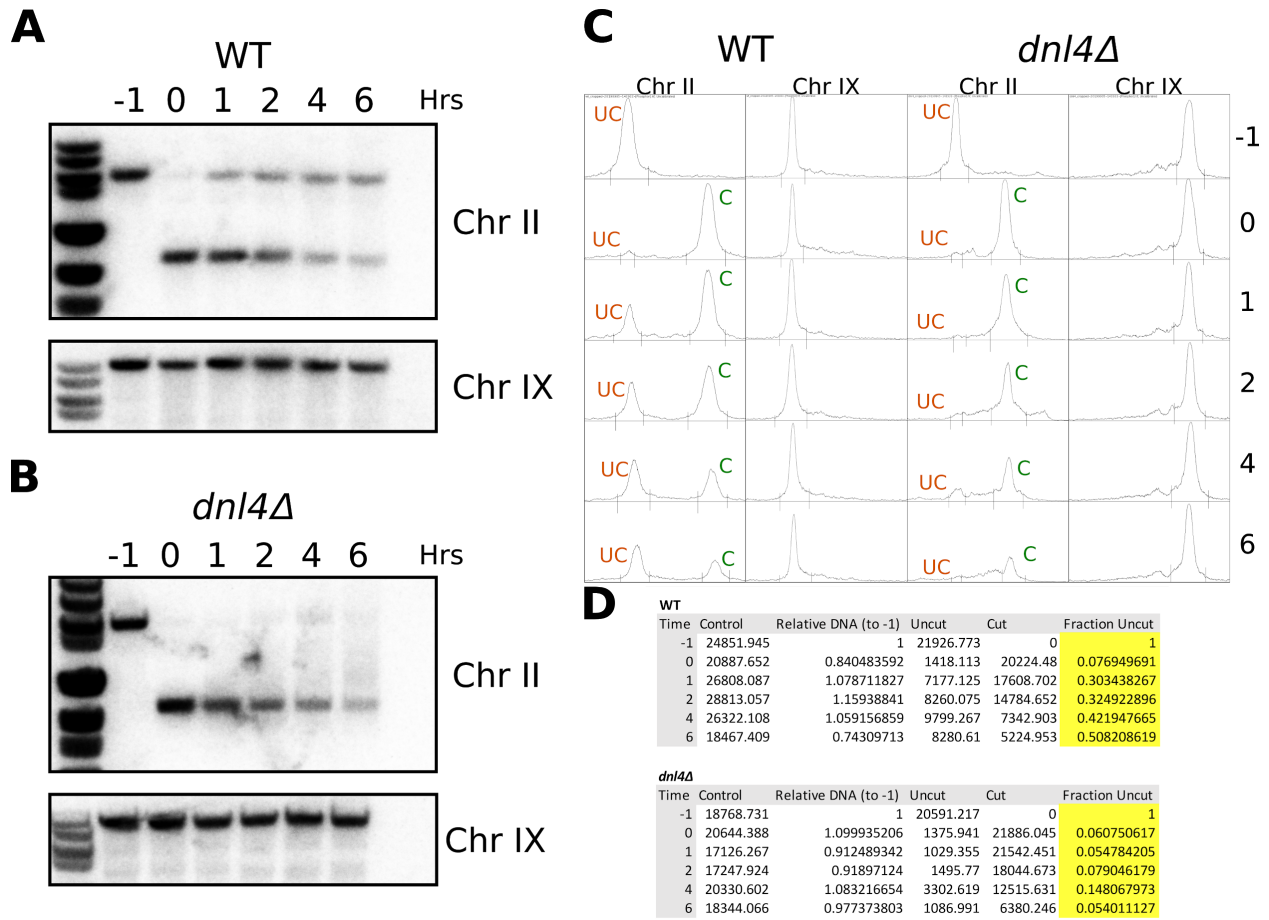
Supplemental Figure 7. Zoomed-in view of genome wide chromatin occupancy plots (GCOPs) of the WT (A), *yku70Δ* (B), and *mre11Δ* (C) strains.



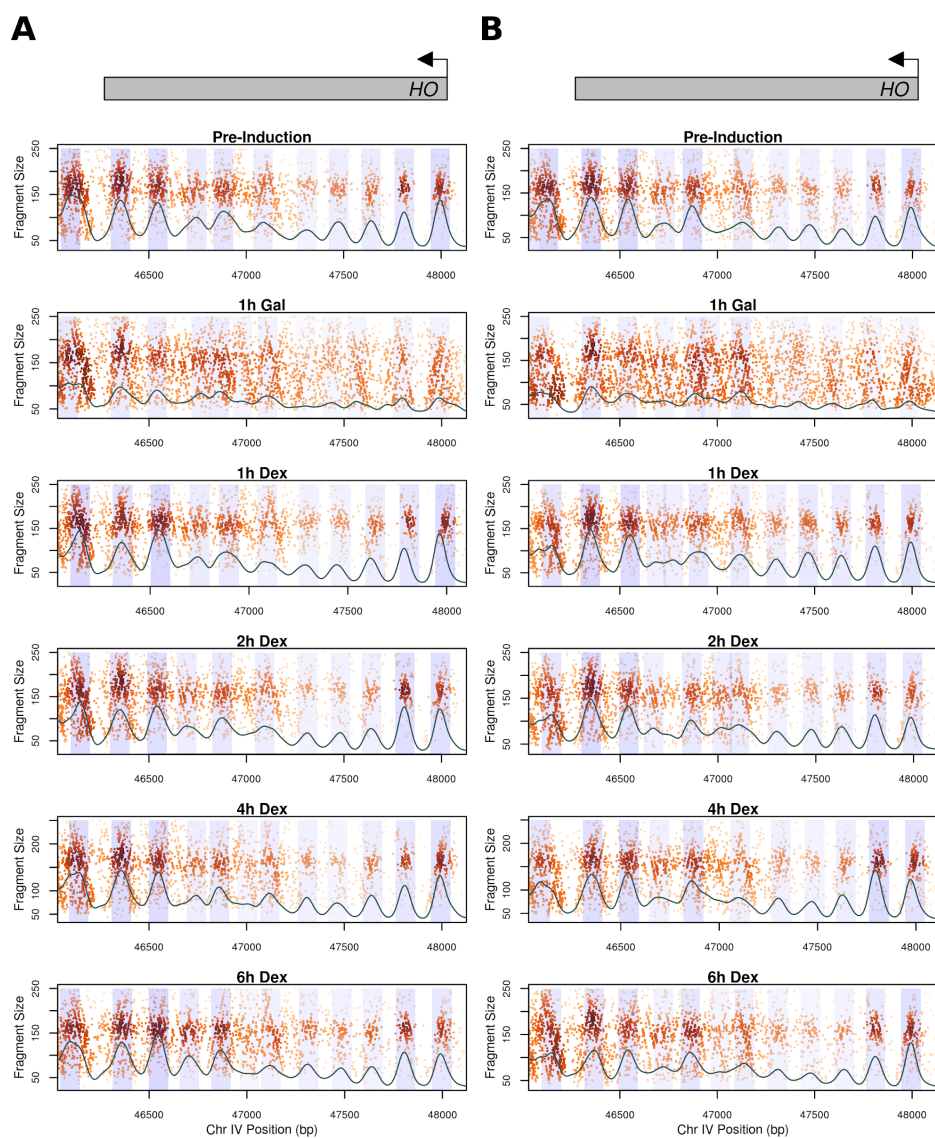
Supplemental Figure 8. Genome wide genic nucleosome analysis in wild type cells following a DSB. The 2D cross correlation score for genic nucleosomes in each time point is expressed as a log₂-fold change relative to the pre-induction state. The coordinates corresponding to the *GAL* loci and the HO induced DSB are annotated on the zoomed in view of Chr II (left panel).



Supplemental Figure 9. Relative nucleosome position and nucleosomal occupancy ~25 kb from the DSB. We detected 307 nucleosomes in a ~50 kb window around the DSB (arrayed on the x axis according to their position) on Chr II and plotted their relative distance to the nearest neighboring nucleosome (in pre-induction) throughout the time course (blue circles). Separately we calculated the occupancy of each individual nucleosome and plotted the log₂-ratio of the 120 min post-induction occupancy to the pre-induction occupancy (red triangles). The dotted green lines denote coordinates 8 kb from the break while the dotted black lines denote 1 kb from the break.

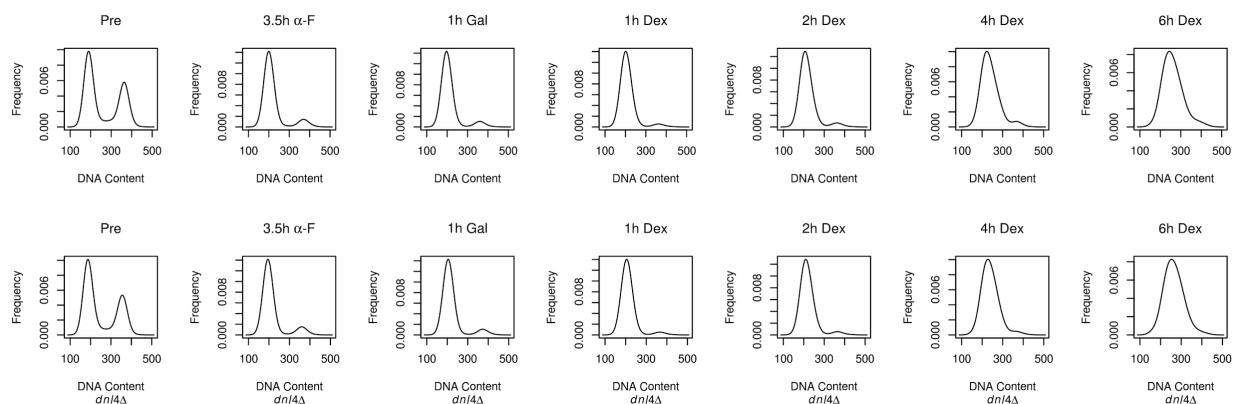


Supplemental Figure 10. Southern Blotting of WT and *dnl4Δ* strains. Southern blots of the WT (A) and *dnl4Δ* (B) strains along with an unrelated control locus from Chr IX. C. Line profiles of each lane that were analyzed in ImageJ to extrapolate uncut (UC, orange), cut (C, green) and control (Chr IX) band intensity. D. Table of the data obtained from the analysis in C, fraction uncut is determined by dividing the uncut signal at each time point by the uncut signal from pre-induction. All of these values are then normalized to the band intensity from Chr IX in the corresponding lane.



Supplemental Figure 11. Genome wide chromatin occupancy plots (GCOPs) of the *HO* gene body in the WT (A) and *dnl4Δ* (B) strains over the NHEJ time course. Gray boxes depict gene bodies, with arrows indicating the direction of transcription. A two-dimensional cross correlation with an idealized nucleosome (see Methods) is calculated at every base pair and depicted as a continuous black trace. The peaks of this

cross-correlation analysis represent the most likely position of a locally detected nucleosome and we have shaded ± 0.5 standard deviations of nucleosome position from the center of each detected peak. The intensity of the shaded color is proportional to the cross-correlation score of the nucleosome peak.



Supplemental Figure 12. FACS profiles of the WT (top) and *dnl4Δ* (bottom) strains throughout the NHEJ time course. DNA content is measured on the horizontal axis while cell count is measured on the vertical axis.